The GTP Effector Site of Ornithine Decarboxylase from *Lactobacillus 30a*: Kinetic and Structural Characterization†

Marcos A. Oliveira, Donald Carroll, Lois Davidson,‡ Cory Momany,§ and Marvin L. Hackert*

Department of Chemistry and Biochemistry, University of Texas at Austin, Austin, Texas 78712

Received March 17, 1997; Revised Manuscript Received September 9, 1997⊗

ABSTRACT: A nucleotide effector site of the biodegradative form of ornithine decarboxylase from *Lactobacillus 30a* (OrnDC *L30a*) has been identified. OrnDC *L30a* activity at pH 8.0, where the enzyme is normally inactive, is stimulated by GTP and dGTP and to a lesser extent by GDP but not by ATP, CTP, or UTP. The pH profile indicates that activation by GTP is reflected by an increase in $k_{cat}/K_{M,orn}$ (above pH 6.8), while V_{max} remains constant over the pH range 4.0−9.0. Scatchard plot analysis shows that GTP binds to OrnDC *L30a* at both pH 5.8 (K_D = 0.11 μM) and pH 8.0 (K_D = 1.6 μM), but unexpectedly, half-site binding is observed at the higher pH. The OrnDC *L30a* dodecamer dissociates into dimers at high pH in the presence or absence of GTP. The GTP binding site was located in difference electron density maps using low-resolution X-ray data. This represents a new type of GTP binding site. A model explaining the activation of OrnDC *L30a* by GTP is presented.

Pyridoxal 5′-phosphate (PLP) dependent ornithine decarboxylase regulates a key step in polyamine metabolism. Polyamines are ubiquitous and are required for several cellular processes such as DNA replication and protein synthesis (*1, 2*). Many bacteria contain two types of amino acid decarboxylases, a biosynthetic enzyme which is constitutively expressed and an inducible or biodegradative form which can be induced in rich medium at low pH. Biodegradative ornithine decarboxylase from *Lactobacillus 30a* (OrnDC *L30a*) is induced by low pH and the presence of ornithine and histidine in the growth medium (*3*−*5*). It catalyzes the conversion of ornithine to putrescine and may be important in regulating cellular pH while the biosynthetic form functions in the synthesis of polyamines needed for cell growth (*5, 6*). Biosynthetic and biodegradative OrnDC from *Escherichia coli* have been shown to be actively stimulated by a number of positive effectors, including nucleotides with guanosine triphosphate (GTP) being one of the most effective (*6, 7*).

The regulation of OrnDC *L30a* activity is not well understood. Functionally OrnDC *L30a* shows a remarkable similarity to the eukaryotic enzymes in terms of its activity and inhibition by substrate analogues, in spite of belonging to a different structural class (*8*). The structure determination of a smaller, dimeric, eukaryotic OrnDC is currently in progress (*9, 10*). The eukaryotic enzyme is regulated by GTP (*11*), and we report herein that GTP also stimulates OrnDC *L30a* activity. The characterization of the regulation of OrnDC *L30a* by GTP will further our understanding of how its complex arrangement of multiple domains communicates to carry out decarboxylation. OrnDC *L30a* was sequenced (*12*) and its structure determined by X-ray diffraction methods (*13*). The X-ray structure revealed a "doughnut"-shaped disk as previously observed in negatively stained electron micrographs (*14*). The doughnut is a dodecamer made up of six dimers arranged with 622 point group symmetry (Figure 1a). Each monomer has 730 amino acids arranged in five sequential folding domains (Figure 2). The N-terminal "wing" domain, critical in the assembly of the dodecamer, is a protrusion localized at the surface of the inner cavity of the dodecamer disk (Figure 1). The linker domain is a 61 amino acid residue segment which forms part of the neighboring subunit's PLP binding site and helps to stabilize the dimer. The linker domains are buried upon formation of the dodecamers (Figure 1b). The third domain binds the PLP cofactor. Four groups of PLP-dependent decarboxylases have been identified (*15*), and three of the four groups are believed to utilize this type of PLP binding motif (*8*). The fourth domain is the specificity domain, containing residues necessary for substrate recognition as shown by site-directed mutagenesis (Zhang and Hackert, unpublished results). The C-terminal domain forms a ridge, creating one wall of a 27 Å deep channel at the dimer interface leading to the active site where PLP is linked to Lys 355 through a Schiff base (Figure 3).

Experiments were performed to identify the GTP binding site and characterize its effects on the kinetics and the oligomeric structure of OrnDC *L30a*. Steady-state kinetics were used to study the profile of $k_{cat}/K_{M,orn}$ and V_{max} as a function of pH**.** GTP binding affinity was analyzed by Scatchard plots, and its binding site was localized using low-resolution difference electron density maps. This GTP binding motif is compared to that observed in other GTP binding proteins and found to be distinctly different from that of the *ras* superfamily of GTPases. On the basis of the X-ray structure and the kinetic data presented here, we propose a model for the activation of OrnDC *L30a* at the higher pH's. The model involves features of a switching

† This work was supported by the National Institutes of Health (GM30105) and the Foundation for Research.

* Author to whom correspondence should be addressed. Phone: (512) 471-1105. FAX: (512) 471-8696. Email: m.hackert@mail.utexas.edu.

‡ Present address: St. Mary's Hospital and Medical Cancer Center, Cancer Research Institute, 2525 N. 8th St., P.O. Box 10430, Grand Junction, CO 81502-5543.

§ Present address: Department of Botany and Biochemistry, University of Georgia, Athens, GA 30602.

⊗ Abstract published in *Advance ACS Abstracts,* December 1, 1997.

S0006-2960(97)00605-3 CCC: $14.00

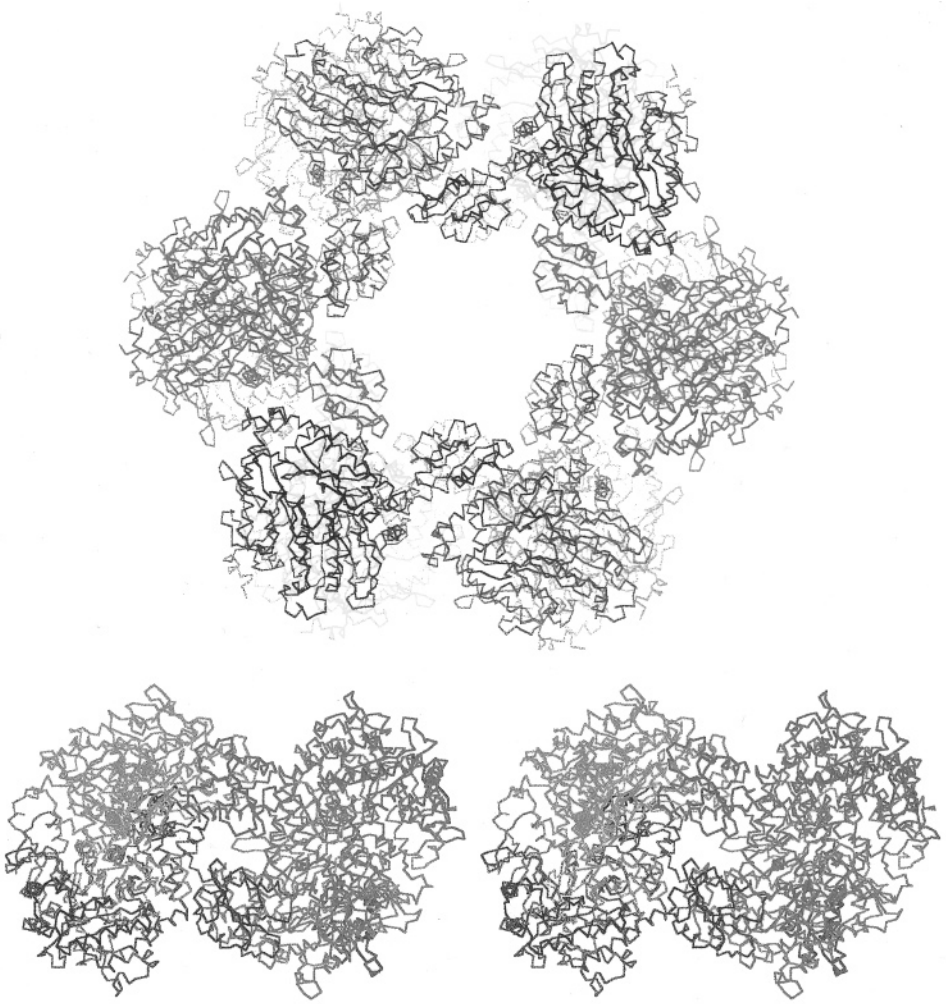

FIGURE 1: (a, top) Cα backbone diagram of the dodecamer of OrnDC *L30a* as observed in the crystalline state at pH 5.8 (*13*). The view shows the doughnut-shaped dodecamer. The dimers interlock above and below through interactions between the protruding wing domain and the linker domain of the neighboring monomer. (b, bottom) A view perpendicular to that shown in panel a, along a 2-fold axis relating two dimers, viewed from the center of the dodecamer. This figure shows that there is no interaction between the top and bottom wing domains.

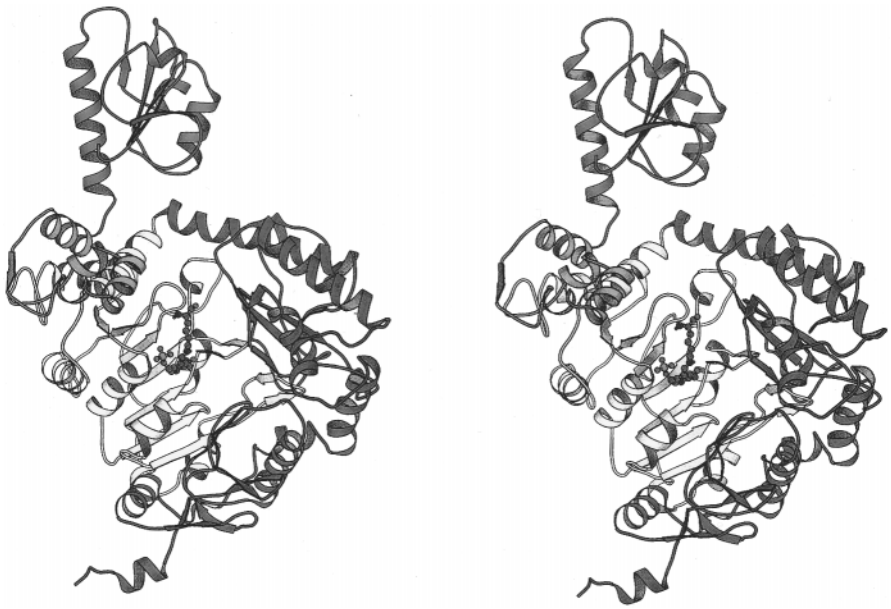

FIGURE 2: Stereo Molscript ribbon drawing of the OrnDC *L30a* monomer indicating in different colors the five domains within the 730 amino acid subunit. Shown in red is the protruding wing domain, in orange the invasive linker domain, in yellow the PLP-binding domain, in green the specificity domain, and in blue the C-terminal domain.

mechanism similar to that described in GTPases. It is proposed that GTP is involved in the stabilization of a linker domain, resulting in reactivation of the enzyme. The half-site binding characteristics of GTP observed at high pH are

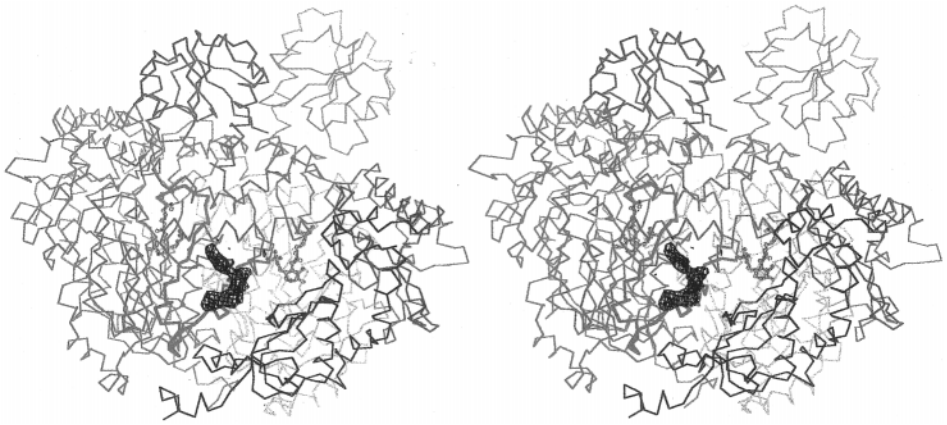

FIGURE 3: Stereo Cα carbon backbone trace of the OrnDC *L30a* dimer, in an orientation similar to that of Figure 2. One monomer is shown in pink, and the 2-fold related monomer has its domains colored according to the scheme adopted in Figure 2. GTP is bound to the surface of one monomer along the subunit interface at the entrance to a deep cavity leading to the active site containing the PLP cofactor, about 27 Å away. A molecular 2-fold axis (roughly vertical) relates the two PLP cofactors shown as ball and stick models. The GTP difference electron density based on 3.9 Å resolution data is also shown.

consistent with the theory of Koshland, Nemethy, and Filmer (KNF) (*16*, *17*) where a ligand (e.g., GTP) induces conformational changes that have unfavorable effects (negative cooperativity) on the binding of a subsequent ligand.

MATERIALS AND METHODS

Bacterial Strain and Growth Conditions. Lactobacillus 30a cells were grown in 14 L batches as described previously (*4*) with minor modifications (*18*). Cells were harvested using a Millipore HVLP 0.45 mm Durapore coarse screen filter in a Pellicon cassette system to concentrate the cells, centrifuged in a GS3 rotor (Sorvall) at 6500 rpm for 20 min at 4 °C and frozen at −20 °C.

OrnDC L30a Purification. OrnDC *L30a* was purified as previously reported (*5*) with a few modifications. After the initial ammonium sulfate precipitation step, a precipitation step with 10% poly(ethylene glycol) was added. A Sephacryl S-500HR gel filtration column was substituted for the Bio-Gel A-1.5 M column.

Assay of OrnDC L30a. Enzyme assays were performed using a Gilson differential respirometer according to the procedure of Guirard and Snell (*5*).

Binding of [^{3}H]GTP to OrnDC L30a. The binding of [8,5′-^{3}H]guanosine 5′-triphosphate (tetrasodium salt, 33 Ci/mmol) was performed in a five-cell equilibrium dialyzer using the method described in Rosen *et al*. (*19*, *20*). Each cell was divided by a 47 mm diameter Spectra Por no. 2 membrane. The left half was filled with 1 mL of the appropriate concentration of [^{3}H]GTP in buffer A (50 mM potassium phosphate buffer, pH 5.8 or pH 8.0, with 0.5 mM EDTA and 0.5 mM dithiothreitol). The right half contained 1 mL of a 0.1 mg/ml solution of OrnDC *L30a* in buffer A. Two 100 μL aliquots of the [^{3}H]GTP solution were removed and counted to provide a zero-time point sample. The binding reaction proceeded for 3.5 h at room temperature while the cells rotated at 20 rpm. The 1 mL solution was removed from each cell half and treated with 240 units of calf alkaline phosphatase for 20 min. The two 100 μL zero-time samples were each treated with 24 units of calf alkaline phosphatase for 20 min. The two 100 μL zero-time samples, plus duplicate 100 μL samples taken from each cell half after 3.5 h dialysis, were placed into 10 mL of counting solution and counted in a Beckman LS 5OOOCE scintillation counter. The membrane from each cell was also counted to determine if any [^{3}H]GTP had bound to it. Three trials were performed for each point for both pH 5.8 and pH 8.0, and the determinations were rotated among the five cells so that each point was not run in the same cell repeatedly. These trials were averaged, and a Scatchard plot was prepared with the standard error of the mean bar included for each point.

pH Profile. Three different buffers were used for the pH profile data. For pH 3.0−5.0, 50 mM sodium acetate buffer was used, for pH 5.5−9.0, 50 mM potassium phosphate buffer was used, and for pH 9.0−12.0, 50 mM sodium bicarbonate was used, all buffers containing 0.5 mM EDTA and 0.5 mM DTT. About 2.5 μg of native OrnDC *L30a* was assayed for each pH point in the presence or absence of 0.1 mM GTP. The integrity of the enzyme at extremes in pH was checked by incubating 2.5 μg of OrnDC *L30a* at pH 3 and 11 for 30 or 60 min, followed by assays in the presence and absence of 0.1 mM GTP at the incubation pH and at the pH optimum, pH 5.8. The V_{max} and $K_{M,orn}$ values for ornithine were determined at pH 4.0, 4.5, 5.0, 5.8, 6.5, 7.4, 7.6, 8.0, 8.7, and 9.4 in the presence of 0.1 mM GTP and at pH 4.0, 4.5, 5.0, 5.8, 6.5, 7.4, and 7.6 in the absence of GTP. Enzymatic assays were carried out as described above. Kinetic parameters were calculated from least-squares fits of the initial activity data plotted according to the methods of Lineweaver−Burk. The plots of log(k_{cat}/$K_{M,orn}$) vs pH were fitted for the loss of one or two protons using programs kindly provided by Dr. W. W. Cleland.

pH and GTP Effects on the Oligomeric State. The size of OrnDC *L30a* was determined by HPLC size exclusion chromatography (SEC) using a ProteinPak 300SW (7.8 × 300 mm) column. The eluant, 50 mM potassium phosphate buffer at pH 5.8 or 7.8, was monitored at 280 nm. OrnDC *L30a* (70 μg) was incubated for at least 15 min at pH 5.8, 6.8, 7.3, and 7.8 in the presence or absence of 0.1 mM GTP before being injected onto the column. The column was calibrated using the Bio-Rad gel filtration standards (Figure 4).

Location of the GTP Binding Site. Crystals of OrnDC *L30a* were obtained by vapor diffusion from poly(ethylene glycol) solutions using the hanging drop method (*18*). Crystals incubated in the presence of GTP at low pH 5.8 shattered, suggesting that a conformational change occurs

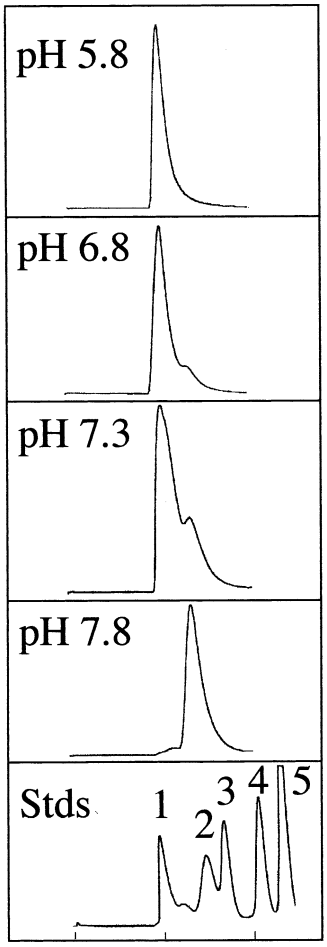

FIGURE 4: Elution profile of the HPLC size exclusion chromatography of OrnDC *L30a* at different pH's showing the transition from a dodecamer (~10^6 Da) at pH 5.8 to a dimer (162 kDa) at pH 7.8. The presence of GTP did not alter the elution profiles. The bottom panel shows the elution profile of gel filtration standards: (1) thyroglobulin (670 000), (2) bovine γ-globulin (158 000), (3) ovalbumin (44 000), (4) myoglobin (17 000), and (5) vitamin B_{12} (1350).

upon binding of GTP. However, an isomorphous crystal grown in the presence of 0.1 mM GTP was able to provide a low-resolution data set collected using a San Diego multiwire detector. The GTP model was fitted to its difference density using the program *O* (*21*). The coordinates of other GTP binding proteins were downloaded from the PDB database and superimposed onto the GTP binding site of OrnDC *L30a* using routines in *O*.

RESULTS

Purification of OrnDC L30a. OrnDC *L30a* was purified to homogeneity as evidenced by the appearance of a single band of the appropriate size on a 10% SDS−polyacrylamide gel after staining with Coomassie brilliant blue. The purity of OrnDC *L30a* was further verified by the appearance of a single band on an isoelectric focusing gel.

Activation of OrnDC L30a by GTP. The purified OrnDC *L30a* was assayed in the presence of a single high concentration (0.1 mM) of different nucleotides at pH 5.8 and 8.0. In each trial about 2.5 μg of OrnDC *L30a* was assayed. Purified OrnDC *L30a* dialyzed against 50 mM phosphate buffer, pH 8.0, is normally inactive. Table 1 summarizes the effects of different nucleotides on the activity of OrnDC *L30a*. At this high concentration none of the nucleotides tested appeared to affect enzymatic activity at pH 5.8, while only GTP, dGTP, and GDP were identified as positive effectors at pH 8.0. The presence or absence of Mg^{2+} in the assay cuvette did not affect the results. Furthermore, when OrnDC *L30a* was assayed in the presence of the nonhydrolyzable analogues for GTP (GTPγS or the GDP−aluminum fluoride monohydrate complex) at pH 8.0, each analogue had the same effect as GTP. These results show that nucleotide binding is necessary and sufficient for enzyme activation at the higher pH values, and GTP hydrolysis is not required.

Table 1: Effect of Nucleotides on OrnDC *L30a* Activity

OrnDC + effector (0.1 mM)	specific activity (μmol of CO_2 min^{-1} mg^{-1})[a] pH 5.8	pH 8.0
OrnDC	180	5
OrnDC + guanine	167	11
OrnDC + guanosine	179	9
OrnDC + GMP	174	22
OrnDC + GDP	175	82
OrnDC + GTP	211	183
OrnDC + dGTP	188	166
OrnDC + 0.1 mM GDP + 0.1 mM AlF_3	211	209
OrnDC + GTPγS		158
OrnDC + GDPβS		98
OrnDC + ATP	187	13
OrnDC + CTP	165	19
OrnDC + UTP	181	8
OrnDC + cGMP	175	4
OrnDC + cAMP	189	2

[a] Estimated errors in specific activities at pH 5.8 and 8.0 are ±11 and ±28 μmol of CO_2 min^{-1} mg^{-1}, respectively.

Table 2: Comparison of GTP Dissociation Constants and $K_{M,orn}$ Values at Different pH Values

	K_D (μM)	$K_{M,orn}$ (mM) +0.1 mM GTP	−GTP
pH 5.8	0.11 ± 0.01	1.0 ± 0.3	1.2 ± 0.4
pH 7.6	ND	1.0 ± 0.3	50 ± 26
pH 8.0	1.6 ± 0.2	1.1 ± 0.3	>500

pH and GTP Effects on the Oligomeric State. Size exclusion chromatography of OrnDC *L30a* at 0.7 mg/mL was performed at different pH's. At the pH optima of 5.8, the dominant species present is the dodecamer. At pH 6.8 a small amount of dimer is present. The percentage of dimer present increases at pH 7.3, and by pH 7.8 the dominant species is the dimer with only a small amount of dodecamer present (Figure 4). A similar distribution of size species was observed over the pH range 5.8−7.8 in the presence of 0.1 mM GTP. These results are confirmed by negatively stained electron micrographs which show the presence of the dodecamer at pH 5.8 but not at pH 8.0.

Equilibrium Dialysis. The purified OrnDC *L30a* was used to analyze GTP binding via Scatchard analysis. Different concentrations of tritiated GTP were dialyzed against the pure OrnDC *L30a* as outlined in Materials and Methods. GTP was found to bind to the OrnDC *L30a* at both pH 5.8 and pH 8.0, but the binding affinity at pH 8.0 was found to be 15-fold less than that observed at pH 5.8 (Table 2). The results of the Scatchard plot (Figure 5) showed that at pH 5.8 there are about 12 independent binding sites per dodecamer, consistent with the known dodecameric stoichi-

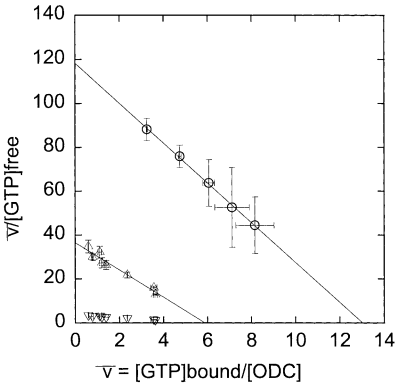

FIGURE 5: Scatchard plot and analysis for the binding of GTP to OrnDC *L30a* at pH 5.8 (○) and pH 8.0. For clarity, the data obtained at pH 8.0 (▽) has been reploted (△) by multiplying the ordinate values by a factor of 10. The marked difference in slopes reflects the lower binding affinity at the higher pH. The microscopic dissociation constant is estimated to be 0.11 μM at pH 5.8 and 1.6 μM at pH 8.0. The value of *n* obtained from the pH 5.8 data is in good agreement with the known dodecameric structure of OrnDC *L30a* while the data at the higher pH shows weaker binding and possibly only one binding site per dimeric unit. The error bars show the standard deviation of the average of triplicate samples assayed on 3 different days in three different dialysis cells.

ometry. It is interesting to note that the apparent number of binding sites at the higher pH corresponds to only half of the sites available, the equivalent of six per dodecamer (or one per dimer since it is known that dissociation to dimers occurs at low protein concentration at higher pH). This result is surprising in light of the observed symmetry between monomers determined from the low pH X-ray structure (*13*).

pH Profile of OrnDC L30a and OrnDC L30a + GTP. The variation of V_{max} and $k_{cat}/K_{M,orn}$ for purified OrnDC *L30a* was measured over a range of pH's from 4.0 to 9.4. V_{max} remains essentially constant over this pH range in the presence or absence of GTP (Figure 6a). Although enzyme activity is lost by incubating OrnDC *L30a* at the extreme pH values of 3 and 11, this can be reversed by reequilibrating the enzyme at the pH optimum of 5.8, indicating the reversible nature of these changes. In the absence of GTP, the $K_{M,orn}$ of 1.0 ± 0.3 mM at the pH optima increases more than 40-fold as the pH is decreased to 4.0 or increased to 7.6 (Table 2). The stimulation of OrnDC *L30a* by GTP at the higher pH range is reflected by a decrease in $K_{M,orn}$ (or increase in $k_{cat}/K_{M,orn}$) above pH 6.8 (Figure 6b) and the extension of the plateau of $k_{cat}/K_{M,orn}$ between the pH range of 6.8−8.0. GDP as well as GTP can also activate OrnDC *L30a* as shown by assays done at pH 7.6 where the enzyme is about 25% active. K_{GTP} for half-maximal activation is 0.43 μM, and K_{GDP} is 1.2 μM at pH 7.6. This value for K_{GTP} is in good agreement with the K_D's obtained by equilibrium dialysis at pH 5.8 and 8.0 described above. The behavior of log($k_{cat}/K_{M,orn}$) vs pH for OrnDC *L30a* in the presence and absence of GTP is illustrated in Figure 6b. The data were analyzed by fitting programs furnished by Dr. W. W. Cleland. In the absence of GTP, the best model requires a slope of 2 at both low and high pH's. Attempts to fit the data with a model assuming the loss of a single proton results in very large errors (>3.5) in the calculated pK_a values. Thus the loss of two protons at low pH, with pK_a's of 4.8 ± 0.2, is required to form the productive ES complex, and the loss of two additional protons, with pK_a's of 6.7 ± 0.1, decreases production of the ES complex. In contrast, in the presence

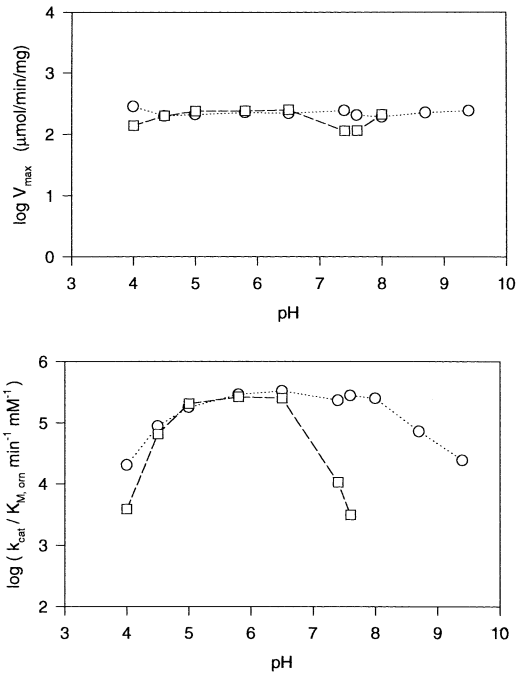

FIGURE 6: (a, top panel) Variation of log V_{max} vs pH for OrnDC in the presence (○) and absence (□) of 0.1 mM GTP. (b, bottom panel) log($k_{cat}/K_{M,orn}$) vs pH for OrnDC and OrnDC + GTP. The slope at low pH is nearly 0.5, indicating the loss of two protons for enzymatic activity. The slope at higher pH is nearly 1, indicating that the titration of a group with a pK_a of 6.5 (−GTP) or 8.0 (+GTP) causes loss of OrnDC *L30a* activity.

of GTP the data can be fit well assuming the loss of a single proton at both ends of the bell-shaped pH profile, corresponding to groups with pK_a values of 5.1 ± 0.1 and 8.2 ± 0.1.

Location of the GTP Binding Site. Crystals grown in the presence of 0.1 mM GTP at pH 5.8 were isomorphous to native OrnDC *L30a*. An X-ray data set was processed to 3.5 Å with an R_{merge} of 8.3% for a total of 257 462 reflections collected of which 26 483 are unique. A difference electron density map calculated to 3.9 Å resolution (Figure 3), using phases of the native OrnDC *L30a* structure at pH 5.8 (*13*), was useful in locating the GTP binding site at the lower pH. Even at this resolution, the *anti* conformation of the nucleotide with extended triphosphate is readily apparent (Figure 3). The nucleotide binds on the surface of the enzyme, 27 Å away from the PLP cofactor, at the entrance to the active site and dimer interface. Each subunit has a separate binding site for the cofactor and effector.

DISCUSSION

We have shown that GTP, and to a lesser extent GDP, activates OrnDC *L30a* in the pH range 6.8−8.0 where OrnDC *L30a* activity normally decreases with increasing pH. The results also indicate that GTP binding, but not hydrolysis, is necessary and sufficient for activation. GTP binds to OrnDC *L30a* at low and high pH's, but at high pH, where GTP exerts its stimulatory effects, only half of the available sites are occupied (Figure 5). The stimulation, reflected as an extension of the pH profile for enzyme activity from 6.8 to 8.0, is a result of changes in $k_{cat}/K_{M,orn}$ while V_{max} remains constant (Figure 6). The pH profile of the enzyme in the presence of GTP shows that a single proton, instead of two protons in its absence, is lost at the low and high ends of

the bell-shaped pH profile (Figure 6b). Protons lost at the lower pH are responsible for enabling the formation of an active ES complex, while the further loss of protons at the higher pH causes loss of enzyme activity. The oligomeric state of the enzyme was also shown to be dependent on pH, going from a dodecamer at low pH to a dimeric species at pHs above 7.5 (Figure 4).

The pK_a values of prototropic groups of the active site can often be determined by measuring the pH dependence of V_{max} and $k_{cat}/K_{M,orn}$. One can suggest that the loss of a single proton at both ends of the pH profile curve (pK_a 5.1 and 8.2, respectively) in the absence of GTP would likely correspond to carboxylic and amino groups in the active site. However, since pH affects groups in the enzyme and substrate as well as the stability of the enzyme, these must be taken into consideration when assigning the identity of the groups reflected in the observed pK_a's (Figure 6b). OrnDC *L30a* is active over a broad range of pH values, and its active site is in a secluded environment buried ~27 Å from the surface of the dimer. Inhibitor studies (Oliveira, Kern, and Hackert, unpublished results) indicate that the active site closes upon substrate binding, which likely contributes to the perturbation of pK_a values of active site groups. In addition, the enzyme dissociates into dimers (Figure 4) with a pK_a (~7.5) close to the pK_a of enzyme inactivation (6.7). This scenario makes it difficult to make any definitive correlation between pK_a's obtained from the pH profile and potential active site groups.

An examination of the dodecamer structure reveals potential side-chain interactions at the wing−linker domain interface sensitive to pH changes. This interface is the result of the interaction between the N-terminal protruding domain (wing) of a monomer of OrnDC *L30a* with the linker domain of a monomer belonging to a neighboring dimer (Figure 1b). The corresponding wing domain of the neighboring monomer interacts with a third neighboring dimer in the same manner such that six monomers interlock in a circular fashion. A similar interlock occurs between the other monomers related by the molecular 2-fold axis within the dimer. Thus there are two sets of 6-fold related wing−linker domain interactions independent of each other; e.g., there is no interaction between wing domains (Figure 1b). At the interface of the wing−linker domains there are two salt bridges: one, an interdimer salt bridge involving Asp87 and Arg155″,[1] and the other, an intrasubunit ion pair involving His78 and Glu94. The apparent loss of a proton with pK_a ~7.5 results in the dissociation of the dodecamer into dimers. This could be attributed to His78, whose pK_a would be expected to be elevated by the nearby Glu94.

In light of the crystal structure, the results presented here are consistent with a model involving a high-symmetry (622) dodecamer that imposes structural restraints on the linker domain that result from interactions with the neighboring wing domain (Figure 1). This restraint is removed when the dodecamer dissociates into dimers at high pH, giving rise to an altered linker domain conformation and inactive enzyme. According to this model (Figure 7) the binding characteristics of GTP depend on the oligomeric state of the enzyme. At low pH symmetry between subunits is enforced by the wing−linker domain interactions so that the dodecamer retains 12 equivalent GTP binding sites, while at high pH half-site GTP binding is observed. Half-site binding observed here is an extreme case of negative cooperativity in which binding of a second ligand is effectively not observed under the conditions of the experiment.

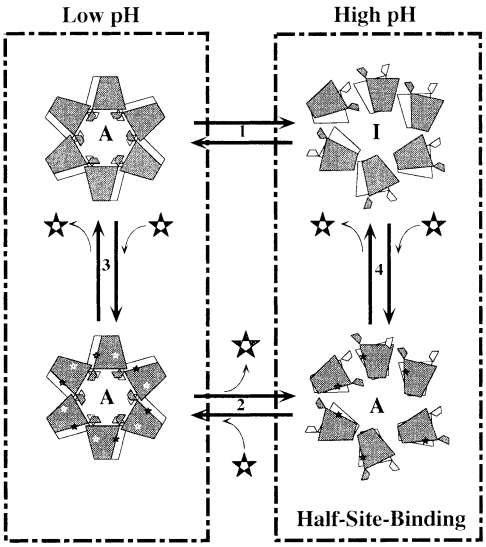

FIGURE 7: Cartoon summarizing the model for the activation of OrnDC *L30a* by GTP (☆). The enzyme undergoes a dissociation from a dodecamer to dimers (**1**, **2**) that is dependent on pH and independent of GTP binding. While the dodecamer is active (A), the dimer formed at high pH is inactive (I). It is proposed that GTP can activate the dimeric form of the enzyme by stabilization of domains that may undergo conformational changes upon dodecamer dissociation. At low pH GTP binds to all 12 sites of the dodecamer (**3**), but there is no effect on the activity of the enzyme. On the other hand, at high pH half-site binding is observed. Half-site binding can be explained by invoking the concept of negative cooperativity in which binding at one site would cause conformational changes detrimental to the binding of GTP at the neighboring site (*16*, *17*).

The structure of OrnDC *L30a* shows a plausible means of communication between the GTP binding sites along the molecular 2-fold axis (Figures 2 and 3). Changes along this interface could lead to an asymmetrical dimer, providing and explanation for the observed half-site GTP binding consistent with the KNF theory (*16*, *17*). A corollary of the model is the prediction of asymmetry between identical monomers that form the dimer. This may not be seen in the crystalline state where the high protein concentration forces the interlock of wing domains, rendering a symmetrical dimer within the dodecamer. A similar situation occurs in crystals of the deoxy form of β4 hemoglobin, which is observed trapped in a R-liganded state (22). However, since in OrnDC *L30a* the 2-fold axis relating the monomers that form a functional dimer (Figure 3) is noncrystallographic, it should be possible to test for an asymmetrical dimer at high resolution (*23*). The initial X-ray structure was determined to 3.0 Å resolution at pH 5.8 and refined with 2-fold restraints. At this resolution no asymmetry was noted (*13*). Small crystals of OrnDC *L30*a at pH 8.0 have been obtained that exhibit the same morphology as displayed by crystals obtained at pH 5.8. This suggests that protein concentrations and conditions conducive for crystal formation will selectively favor symmetrical dodecamers. We are currently testing this model (Figure 7) by mutating residues at the wing−linker interface in order to prevent dodecamers from forming and to generate a dimeric form of OrnDC *L30a.* Our model would predict

[1] Double-primed residues belong to a neighboring dimer.

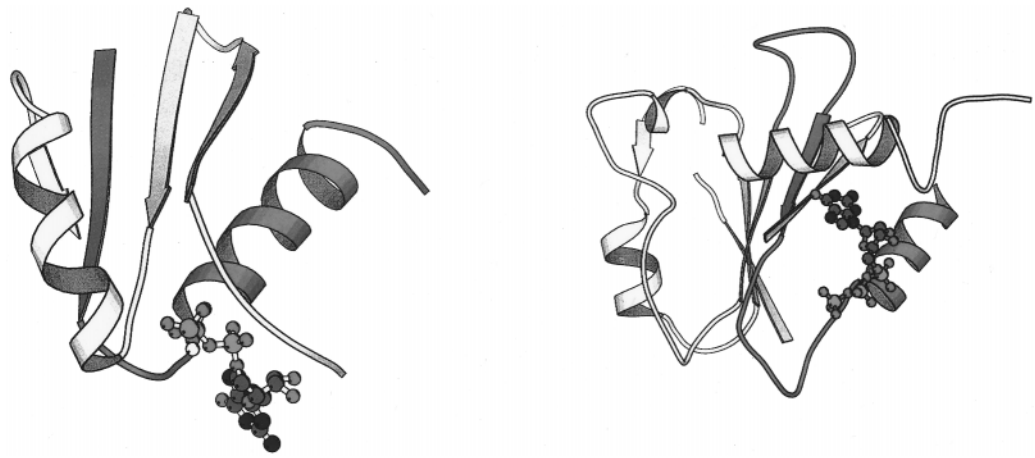

FIGURE 8: Ribbon drawing of five of the seven-stranded β-sheet of OrnDC *L30a* (right) and three β-strands of the G_{ia} structure (left), both with bound GTP. The phosphate binding loop is highlighted in red.

that such a species would be inactive at high or low pH but could be activated by GTP.

The GTP binding site, localized at the entrance of the active site ~7 Å away from a lysine residue at the C-terminal domain, suggests that it may also be involved in stabilizing the "closed" state of OrnDC *L30a*. A closed state has been observed for the related aspartate aminotransferase (*24*) and also for OrnDC *L30a* in inhibitor complexes (Oliveira, Kern, and Hackert, unpublished results). The involvement of GTP in stabilizing the closed form of the enzyme would explain the resulting decrease in $K_{M,orn}$ observed in the dimeric state for pH's above 6.8.

The amino acid sequence of OrnDC *L30a* (*12*) was searched for a consensus GTP binding sequence using the protein sequence patterns compiled in PROSITE (*25*), but none was found. Nonetheless, we were able to show by equilibrium dialysis and low-resolution difference electron density maps that OrnDC *L30a* has a GTP binding site localized at the surface at the dimer interface and near the entrance to the deep cleft that leads to the active site (Figure 3). At this point we can only assume that this tight binding site is also the one used at the higher pH's, but that will need to be confirmed. In the *ras* superfamily of GTPases, elongation factor Tu, and the G-proteins of signal transduction, the GTP binding site is at the C-terminal end of a parallel β-sheet with the second phosphate typically positioned near the positive dipole at the N-terminal end of an α-helix. OrnDC *L30a* contains a large seven-stranded β-sheet (Figure 2). Six of these seven strands run toward the center of the dimer with the cofactor binding site at the C-terminal end of those strands. The remaining strand runs antiparallel to the rest of the sheet toward the surface of the dimer where it makes a short loop before returning via a short α-helix. The second phosphate of the GTP binds near the N-terminal end of this short helix (Figure 3). The nucleotide is bound in the *anti* conformation reminiscent of GTP conformation observed for other G-proteins (*26, 27*). However, the guanosine portion of the nucleotide is positioned in a very different manner (Figure 8). The presence of this single β-strand and a return helix appear to be the only structural elements in common to the other GTP binding proteins referred to earlier (Figure 8). Furthermore, the amino acid sequence of residues 170−200 that define most of the interactions that bind the G-base of the activator was searched against GenBank using BLAST, with only the bacterial, basic amino acid decarboxylases being identified as matches. Thus this appears to represent another type of GTP binding site not previously reported.

ACKNOWLEDGMENT

The authors gratefully acknowledge Dr. Lawrence Poulsen for helpful comments during the preparation of the manuscript. The authors also gratefully acknowledge the use of the computer programs for the analysis of the kinetic data that were provided by Dr. W. W. Cleland. Figures 2 and 8 were made with MOLSCRIPT (*28*); figures 1 and 3 were made with MOLVIEW (*29*).

REFERENCES

1. Tabor, C., and Tabor, H. (1976) *Annu. Rev. Biochem. 45*, 285−306.
2. Pegg, A. E. (1988) *Cancer Res. 48*, 759−774.
3. Applebaum, D. M., Dunlap, J. C., and Morris, D. R. (1977) *Biochemistry 16*, 1580−1584.
4. Chang, G. W., and Snell, E. E. (1968) *Biochemistry 7*, 2005−2012.
5. Guirard, B. M., and Snell, E. E. (1980) *J. Biol. Chem. 255*, 5960−5964.
6. Anagnostopoulos, C., Choli, T., and Kyriakidis, D. A. (1992) *Biochem. Int. 27*, 991−1000.
7. Holtta, E., Janne, J., and Pispa, J. (1972) *Biochem. Biophys. Res. Commun. 47*, 1165−1171.
8. Momany, C., Ghosh, R., and Hackert, M. L. (1995) *Protein Sci. 4*, 849−854.
9. Kern, A., Oliveira, M. A., Chang, N.-L., Ernst, S. R., Carrol, D. W., Momany, C., Minard, K., Coffino, P., and Hackert, M. L. (1996) *Proteins 24*, 266−268.
10. Grishin, N. V., Osterman, A. L., Goldsmith, E. J., and Phillips, M. A. (1996) *Proteins 24*, 272−273.
11. Kilpelainen, P. T., and Hietala, O. A. (1994). *Biochem. J. 300*, 577−582.
12. Hackert, M. L., Carroll, D. W., Davidson, L., Soo-Ok, S., Momany, C., Vaaler, G. L., and Zhang, L. (1994) *J. Bacteriol. 176*, 7391−7394.
13. Momany, C., Ernst, S., Ghosh, R., Chang, N.-L., and Hackert, M. L. (1995) *J. Mol. Biol. 252*, 643−655.
14. Stoops, J. K., Momany, C., Ernst, S. R., Oliver, R. M., Schroeter, J., Bretaudiere, J.-P., and Hackert, M. L. (1991) *J. Electron Microsc. Tech. 18*, 157−166.
15. Sandmeier, E. Hale, T. I., and Christen, P. (1994) *Eur. J. Biochem. 221*, 997−1002.
16. Koshland, D. E., Nemethy, G., and Filmer, D. (1966) *Biochemistry 5*, 365−385.

17. Koshland, D. E. (1996) *Curr. Opin. Struct. Biol. 6*, 757−761.
18. Momany, C., and Hackert, M. L. (1989) *J. Biol. Chem. 264*, 4722−4724.
19. Spectrum Medical Industries (1980) *Data, Instruction Manual*, pp 1−31.
20. Rosen, D., Okamura, M. Y., and Feher, G. (1980) *Biochemistry 19*, 5687−5692.
21. Jones, T. A., Zou, J. Y., Cowan, S. W., and Kjeldgaard, M. (1991) *Acta Crystallogr. A47*, 110−119.
22. Borgstahl, G. E., Rogers, P. H., and Arnone, A. (1994) *J. Mol. Biol. 236*, 831−843.
23. Kleywegt, G., and Jones, T. A. (1995) *Structure 3*, 535−540.
24. Picot, D., Sandmeier, E., Thaller, C., Vincent, M. G., Christen, P., and Jansonius, J. N. (1991) *Eur. J. Biochem. 196*, 329−341.
25. Bairoch, A. (1992) *Nucleic Acids Res. 20*, 2013−2018.
26. Pai, E. F., Kabsch, W., Krengel, U., Holmes, K. C., John, J., and Wittinghofer, A. (1989) *Science 341*, 209−214.
27. Coleman, D. E., Berghuis, A. M., Lee, E., Linder, M. E., Gilman, A. G., and Sprang, S. R. (1994) *Science 265*, 1405−1412.
28. Kraulis, P. (1991) *J. Appl. Crystallogr. 26*, 283−291.
29. Smith, T. J. (1993) *J. Appl. Crystallogr. 26*, 496−498.

BI970605G